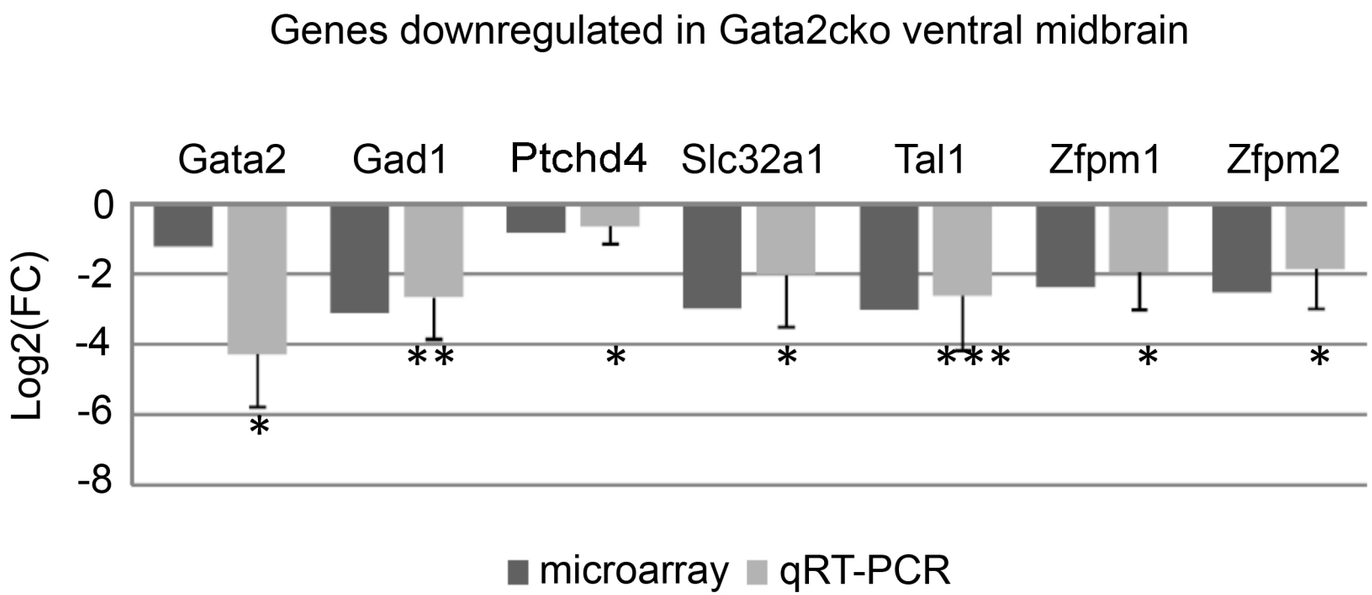

Fig. S1. Comparison of the fold change indicated by the microarray data analysis and quantitative RT-PCR. FC, fold change. For a selection of predicted Gata2-regulated genes, qRT-PCR assay was performed. After RT-PCR, fold change was calculated using the Ct values detected in the *Gata2*^{cko} and control (*En1*^{Cre}*; Gata2*$^{flox/wt}$) cDNA. Samples were normalized against *Actb* expression level in the same sample. The qRT-PCR was performed with 4 replicate cDNA samples. The statistical significance of the fold change in normalized expression levels is indicated. *** P<0.001, ** P<0.01, * P<0.05. The results of the microarray and qRT-PCR are largely consistent. An exception is the *Gata2* gene, where the microarray detects a truncated non-functional transcript.

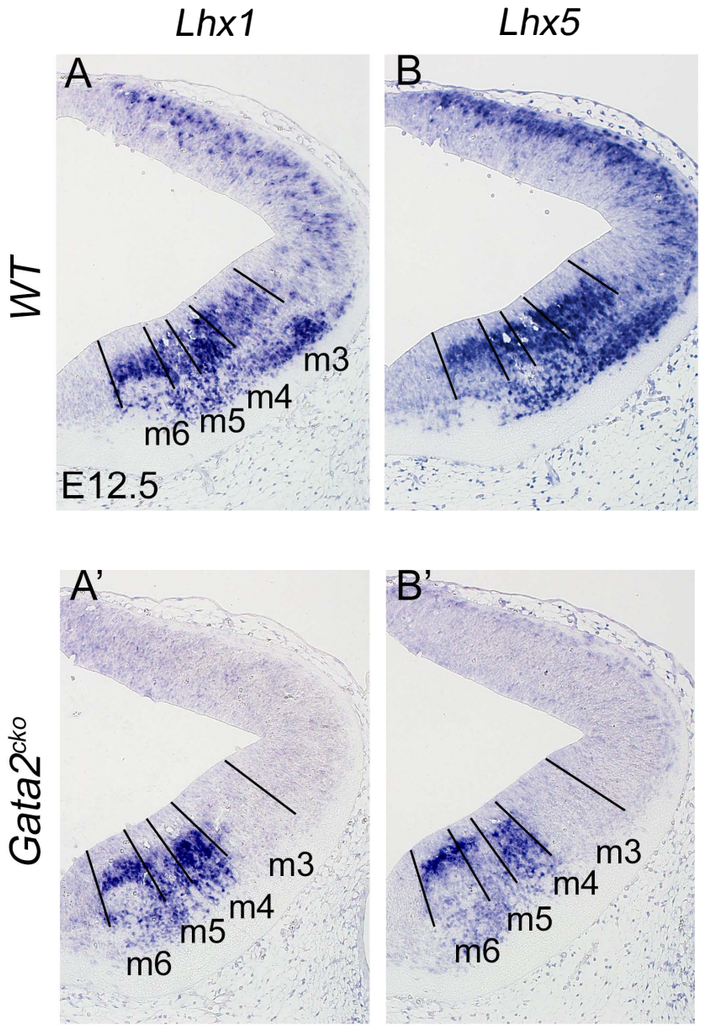

Fig. S2. ISH analysis. (A-B') Lhx1 (A,A') and Lhx5 (B,B') in wild-type and Gata2cko mutant embryos at E12.5.

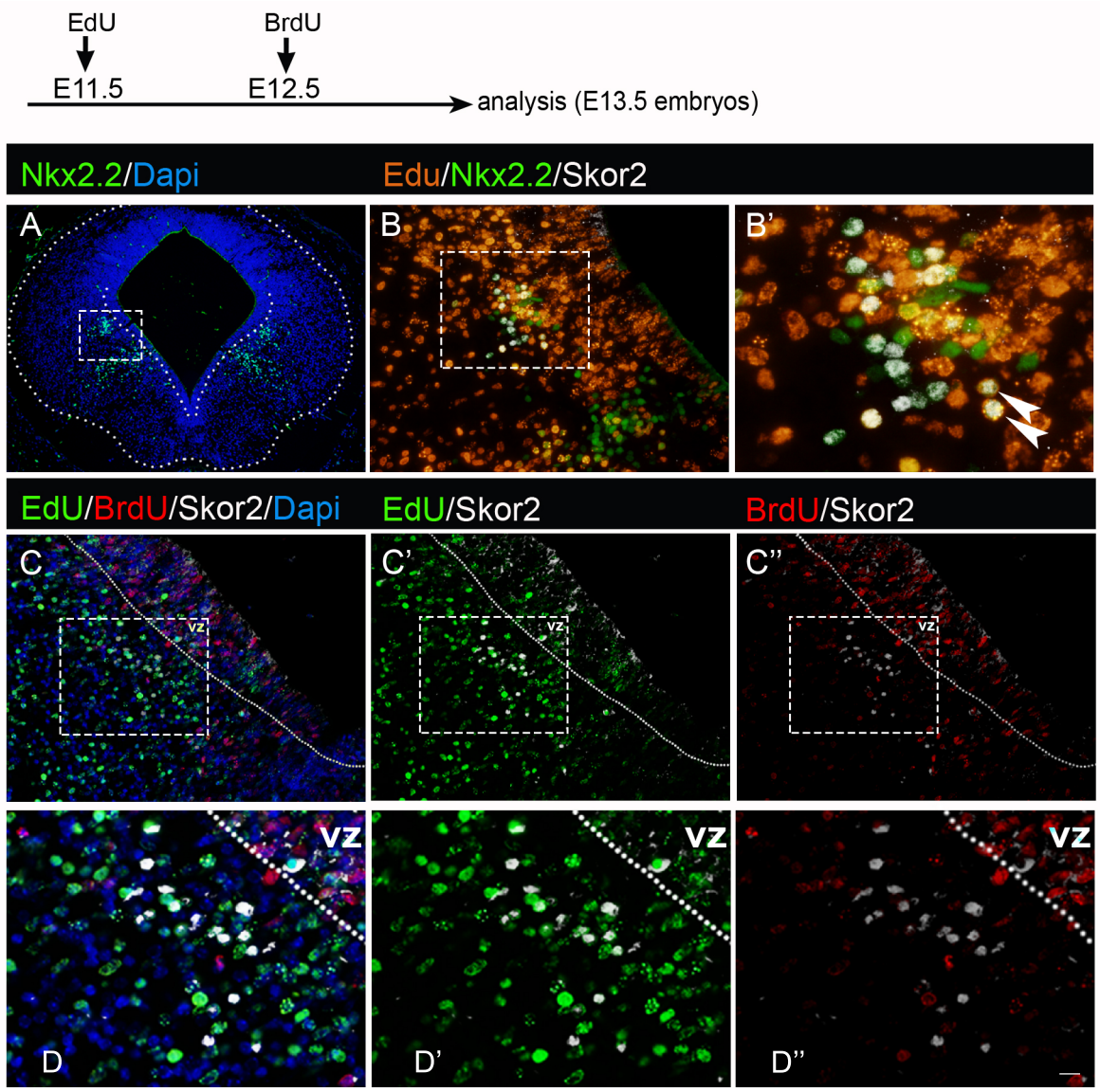

Fig. S3. *Skor2*$^{+}$ neuron birth-dating by BrdU and EdU labelling.

Pregnant females received one dose of EdU at E11.5 and one dose of BrdU at E12.5 of pregnancy. Embryos were dissected at E13.5 and analyzed for the label.

A, Nkx2-2 IHC on a coronal section of the E13.5 mouse midbrain.

B-B', Coexpression of Nkx2-2, Skor2 and EdU in E13.5 mouse midbrain. B', a close-up of Skor2^{+} cells (dashed box in B). Arrowheads indicate triple-labelled cells.

C-D'', Labelling for EdU and BrdU in Skor2^{+} cells. EdU is detected in most of the Skor2^{+} cells (C'). BrdU is not detected in the Skor2^{+} cells (C''). Close-ups of indicated regions are shown in D-D''. vz, ventricular zone.

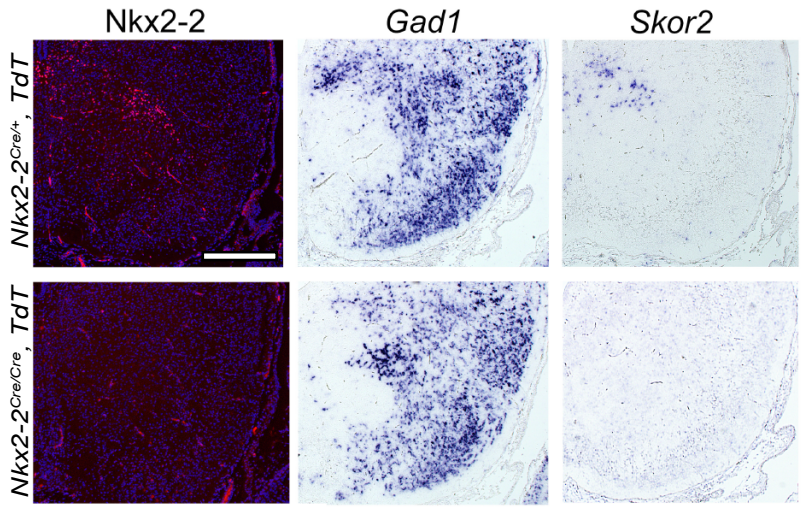

Fig. S4. *Skor2*, but not *Gad1* expression is lost in the *Nkx2-2* mutant mouse.

Coronal sections of E18.5 mouse midbrain analysed for the expression of Nkx2-2 (IHC), *Gad1* and *Skor2* (ISH), in *Ctrl* (*Nkx2-2*$^{Cre/wt}$, *TdT*) and *Nkx2-2*^{null} mutant (*Nkx2-2*$^{Cre/Cre}$, *TdT)* mice. Scale bar: 200 μm.

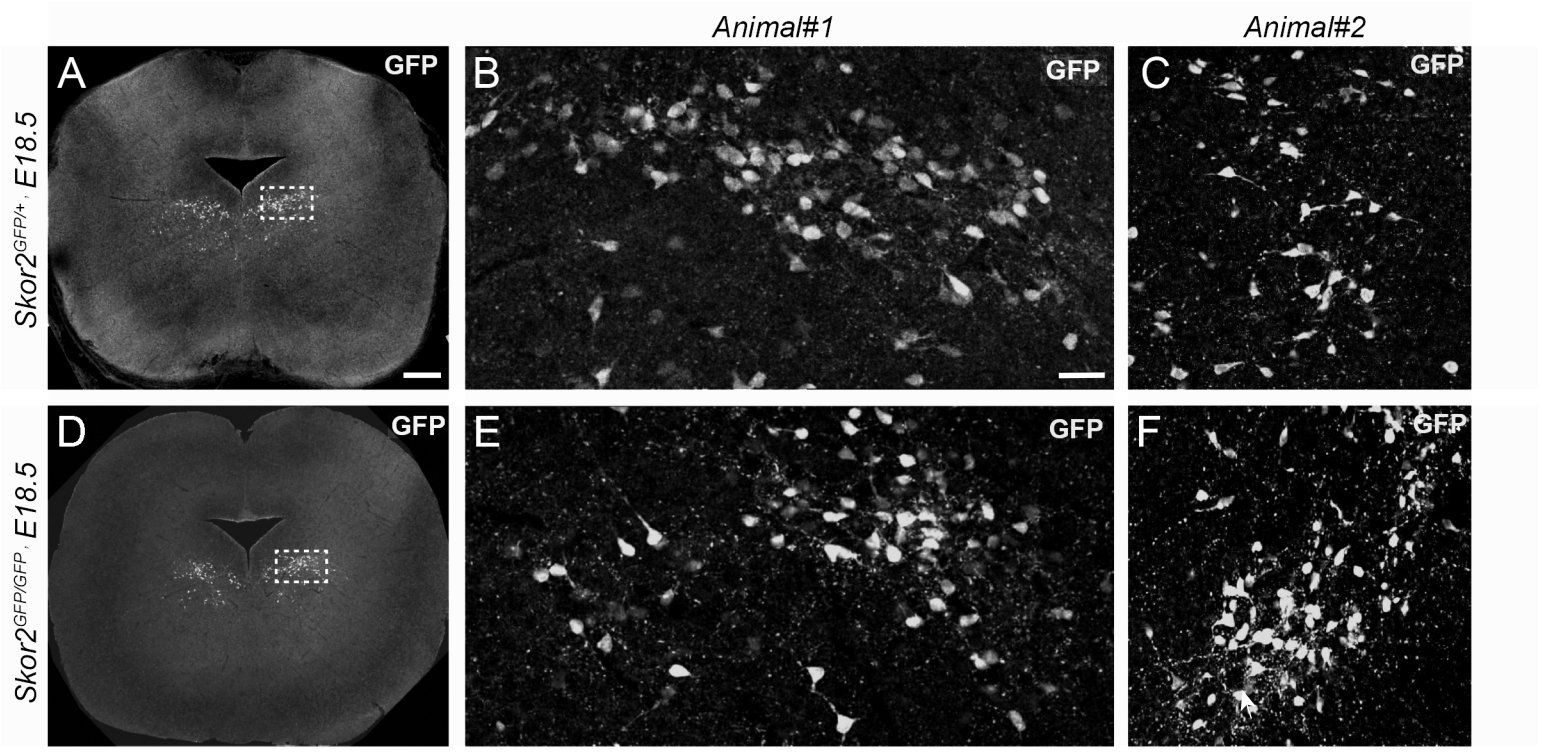

Fig. S5. Normal appearance of neurons expressing the *Skor2* gene is in mice homozygous for a *Skor2* null allele. GFP expression (IHC) on coronal sections of E18.5 *Skor2*$^{GFP/+}$ (A-C) and *Skor2*$^{GFP/GFP}$ midbrain (D-F). The position and number of cells as well as the number and appearance of neurites look similar between the genotypes. Arrowheads point to neuronal projections. Scale bar: 200 μm (A,D), 50 μm (B,C,E,F).

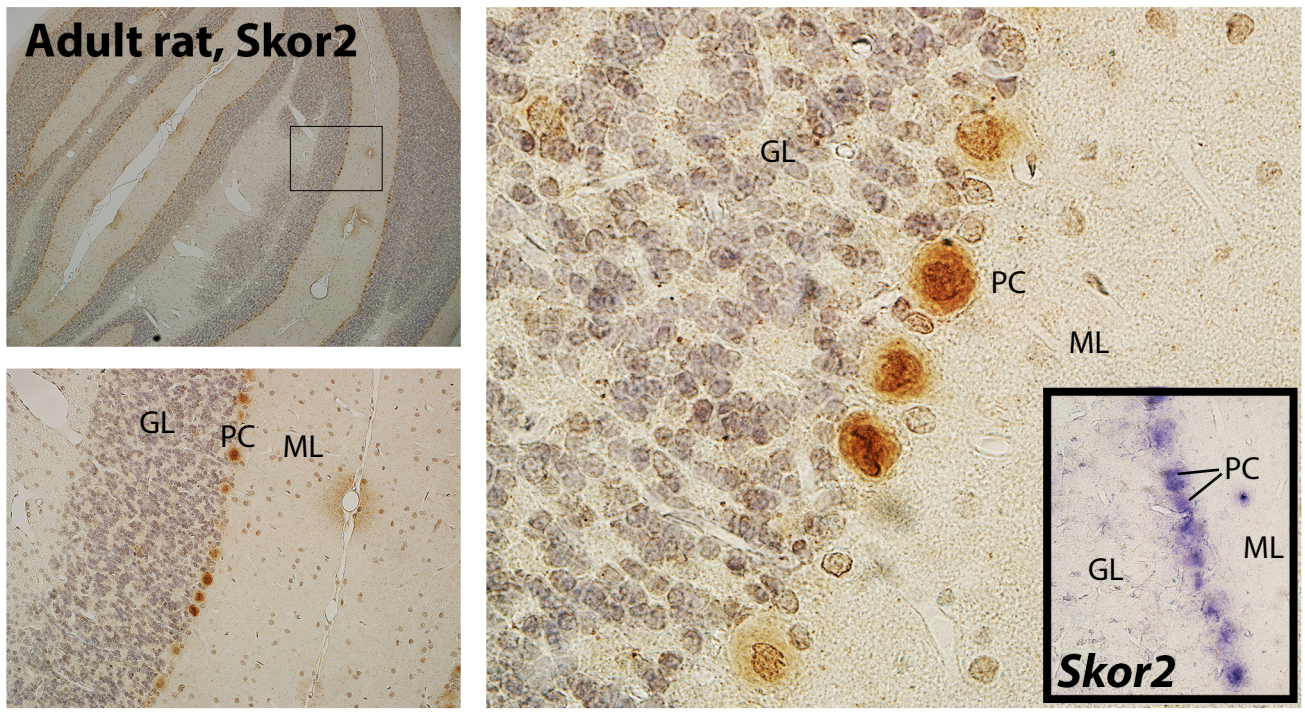

Fig. S6. Skor2 expression in the adult rat cerebellum. IHC and ISH on coronal sections. Skor2 protein was detected in the Purkinje cells (PC) in the rat cerebellum (orange, IHC). The inset shows *Skor2* mRNA expression in the Purkinje cells (violet, ISH). ML, molecular layer; GC, granular layer.

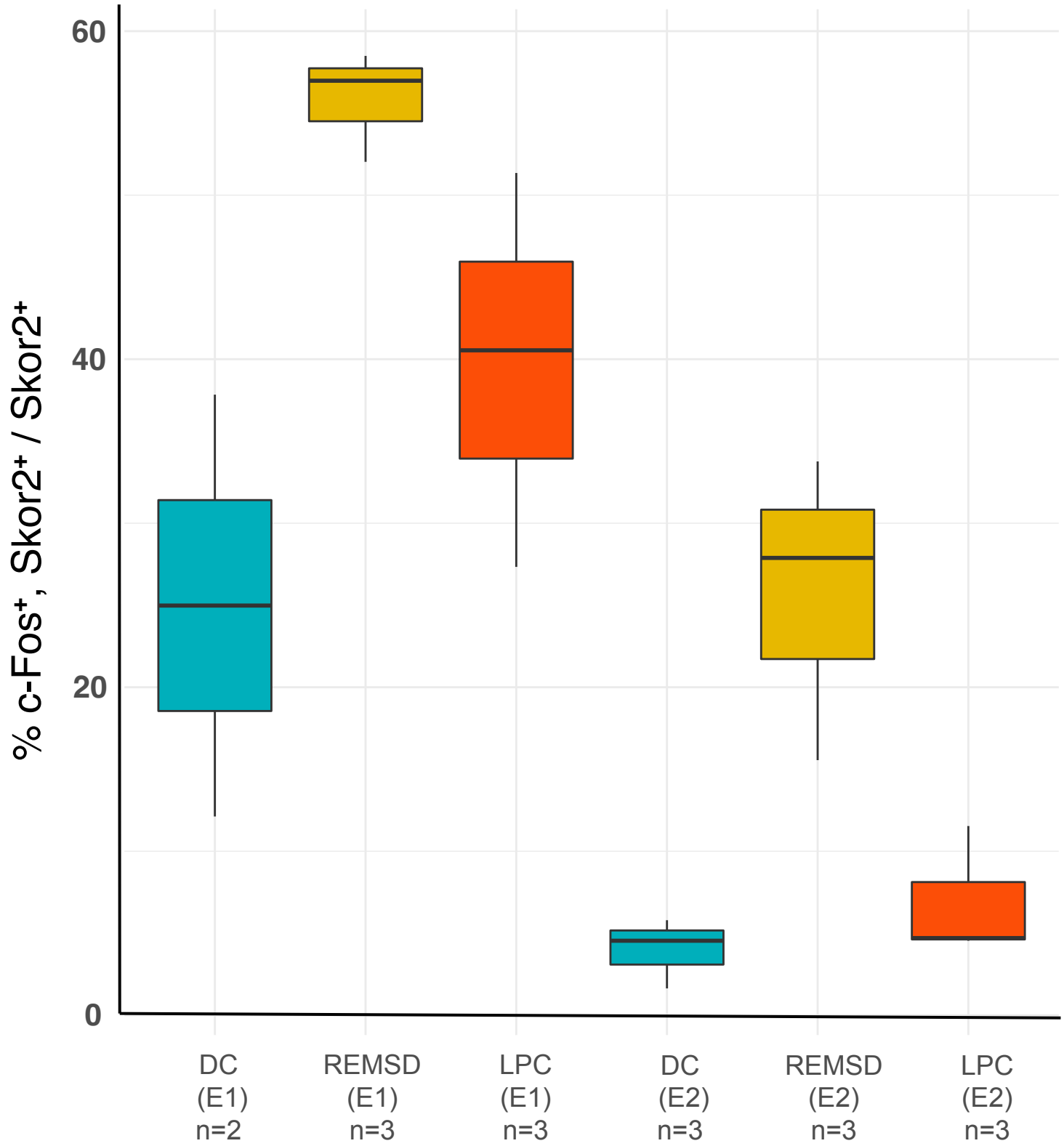

Fig. S7. c-Fos staining efficiency in REM sleep deprivation experiments, before normalisation. Data is presented as percent of c-Fos-positive cells from the dMRF/vlPAG *Skor2*$^{+}$ cells. Experiment groups (DC, REMSD, LPC) and experiment number (E1, E2) is indicated. Due to staining efficiency or other technical variation, the proportion of c-Fos labelled cells differs between the individual experiments (E1 and E2). The difference is systematic, as the experiment groups (DC, REMSD, LPC) show the same trend in labelled cell proportion. The number of animals (n) in each experiment and treatment group is indicated.

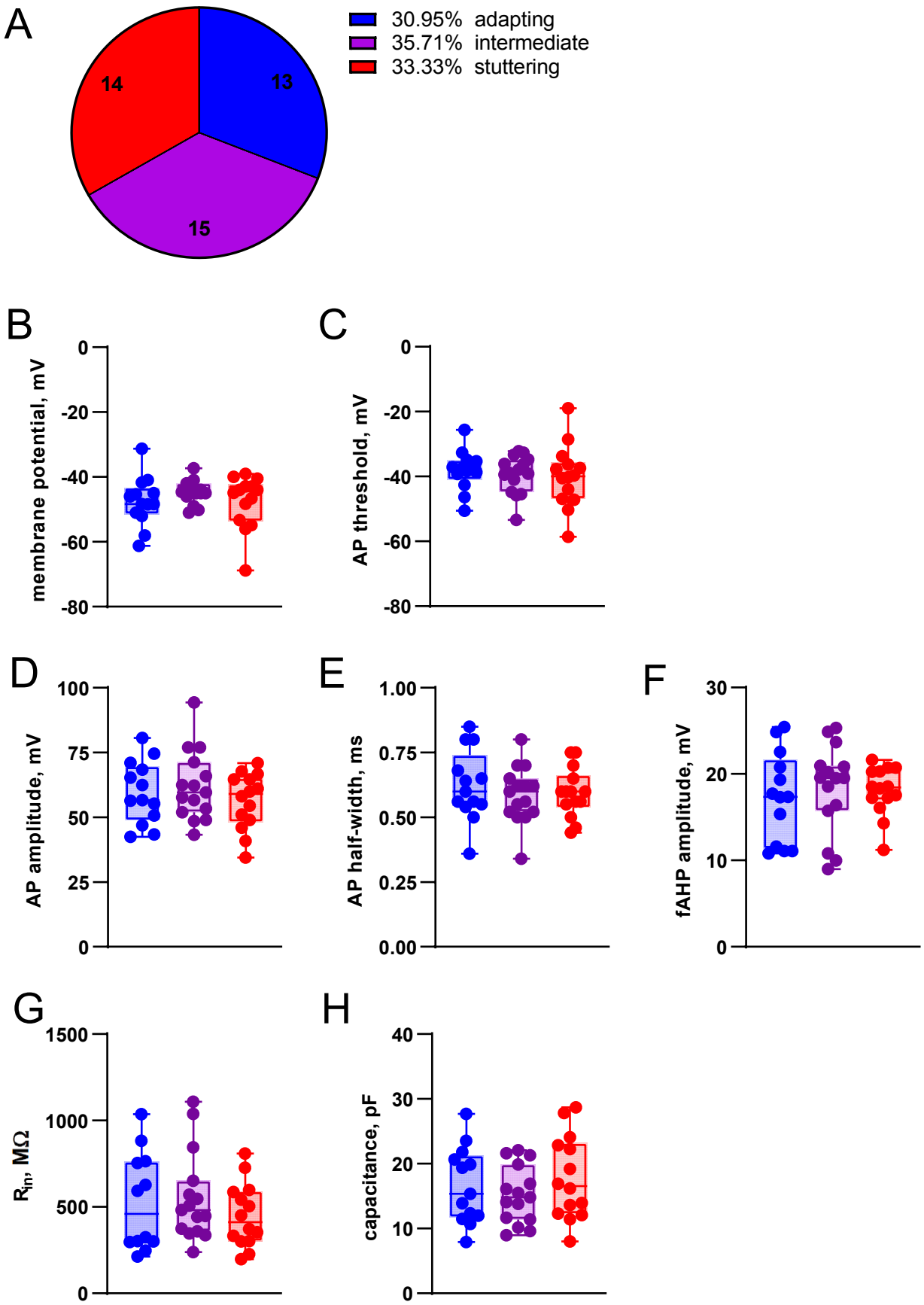

Fig. S8. Classification of the *Skor2*$^{+}$ neurons by the firing patterns. A, The proportion of cells by the assigned firing pattern class. B-H, Comparison of the excitability parameters measured in adapting, intermediate and stuttering GFP^{+} neurons in the *Skor2*$^{GFP/+}$ mouse midbrain by electrophysiology. Boxplots show median, 25 and 75 percentiles with whiskers showing minimum and maximum values. RMP, resting membrane potential; AP, action potential; mAHP and fAHP, medium and fast after-hyperpolarizing potential; R_{in}, input resistance.

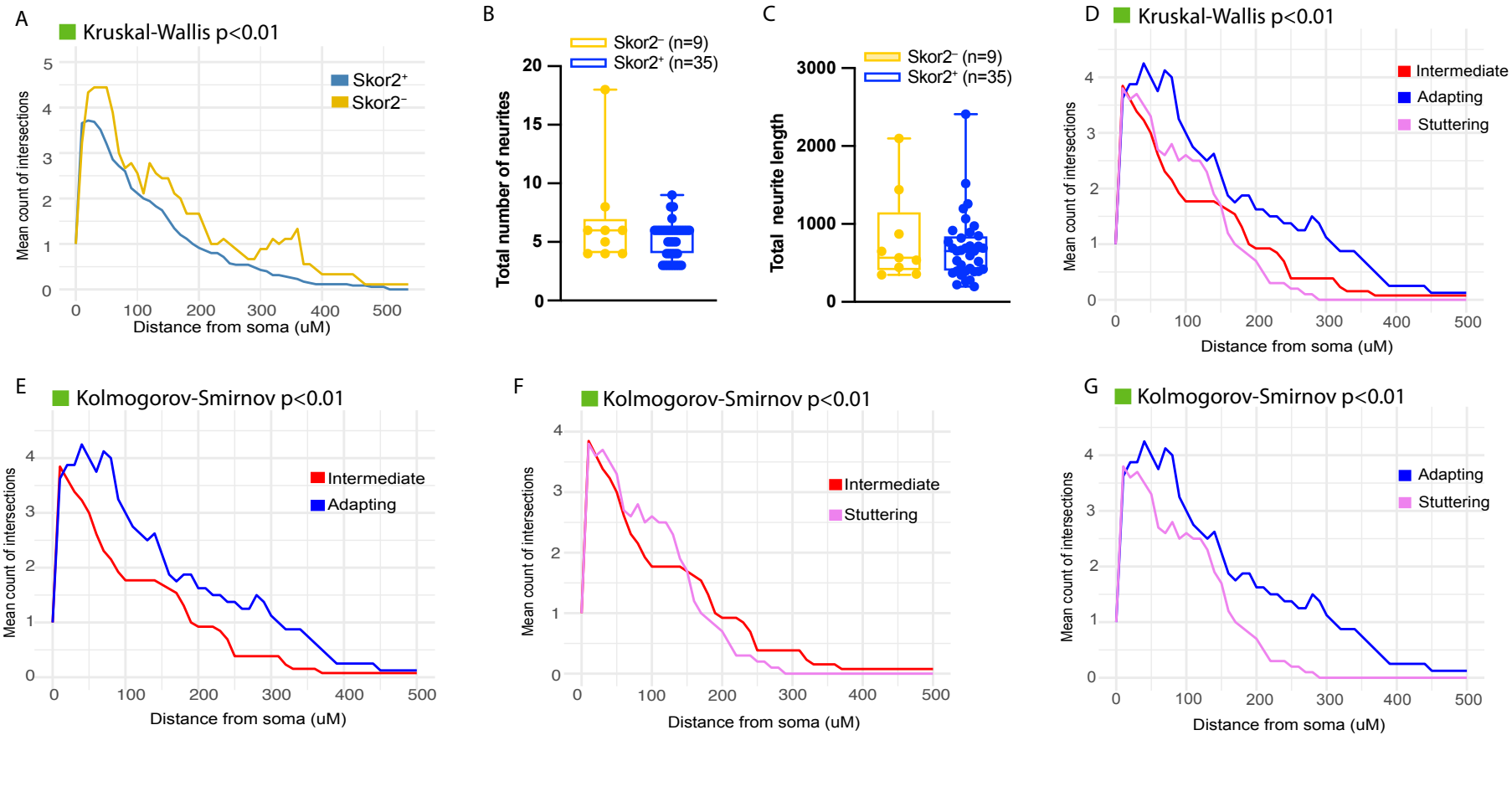

Fig. S9. Comparison of morphological measurements of the *Skor2*+ and *Skor2*- neurons and the *Skor2*+ neuron subclasses

A, Average number of the intersections (+/- SEM) in Sholl analysis of GFP^{+} (*Skor2*$^{+}$, n= 35) and GFP^{-} (*Skor2*$^{-}$, n= 9) cells in the *Skor2*$^{GFP/+}$ mouse midbrain. The distance intervals where significant change (Kruskal-Walls test $p<0.01$) in the number of intersections was observed is highlighted in green. Calculations were conducted with moving window of 50 μm.

B-C, Comparison of the neurite number (B) and length in pixels (C) between the GFP^{+} (*Skor2*$^{+}$, n= 35) and GFP^{-} (*Skor2*$^{-}$, n= 9) cells.

D-G, Average number of the intersections (+/- SEM) in Sholl analysis of GFP^{+} neuron subclasses. The comparative analysis of all three cell classes (D), as well as the pairwise comparisons are shown. The distance intervals where significant change in the number of intersections was observed is highlighted in green. Kruskal-Wallis test of multiple comparisons was used in the comparison of three groups, Kolmogorov-Smirnov test for the pairwise comparison. Significance threshold in both tests was $p<0.01$. Calculations were conducted with moving window of 50 μm.

Table S1. Downregulated genes in the E12.5 *Gata2*^{cko} midbrain.

Click here to download Table S1

Table S2. Complete list of down- and upregulated genes in E12.5 *Gata2*^{cko} dorsal and ventral midbrain, identified in the microarray data analyses.

Click here to download Table S2

Table S3. The gene ontology (GO) terms enriched among the genes downregulated in the *Gata2*^{cko} midbrain. DAVID (https://david.ncifcrf.gov/) was used for the enrichment analysis.

Click here to download Table S3

Table S4. The group identity, experiment ID, number of *Skor2*$^{+}$ cells, number of c-Fos^{+} cells, the percent of c-Fos labelled *Skor2*$^{+}$ cells and the transformed z-scores for each animal in the REM sleep deprivation assay.

Click here to download Table S4

Table S5. Antibodies and mRNA ISH probes used in the study.

Primary antibodies				
Target protein	**Supplier**	**Catalog number**	**Produced in (species)**	**Working concentration**
TH	Millipore	MAB318	mouse	1:500
Ctb	List biological Lab.Inc.	703	goat	1:1000
GFP	Abcam	ab13970	chicken	1:1000
GFP	Abcam	ab290	rabbit	1:500
Neurofilament	DSHB	2H3	mouse	1:500
FoxP1	Abcam	ab16645	rabbit	1:400
Nkx2-2	DSHB	74.5A5	mouse	1:200
Orexin r1 (HCRTR1)	Alomone labs	AOR-001	rabbit	1:100
Orexin r2 (HCRTR2)	Alomone labs	AOR-002	rabbit	1:100
Skor2	Atlas antibodies	HPA046206	rabbit	1:400
Pou4f1(Brn3a)	Santa Cruz Biotechnology	sc-8429	mouse	1:200
RFP	Rockland	600-401-379	rabbit	1:500
c-Fos (FosB)	Abcam	ab11959	mouse	1:500
Secondary antibodies				
rabbit IgG 488	Thermo fisher scientific	A21206	donkey	1:400
rabbit IgG 568	Thermo fisher scientific	A21202	donkey	1:400
goat IgG 568	Thermo fisher scientific	A11057	donkey	1:400
mouse IgG 568	Thermo fisher scientific	A32744	donkey	1:400
mouse IgG 647	Thermo fisher scientific	A31571	donkey	1:400
rabbit IgG 647	Thermo fisher scientific	A31573	donkey	1:400
chicken IgG 488	Thermo fisher scientific	A32931	goat	1:400

mRNA probes		
Target gene	**Source**	**Clone number (if applicable)**
Gad1	RZPD	IRAVp968CM67D6
Gata2	Lilleväli et al., 2004	n/a

Gata3	Lilleväli et al., 2004	n/a
Lhx5	Source Bioscience	IMAGE ID 6830059
Nkx2-2	RZPD	IMAGE clone 480100
Six3	Source Bioscience	IMAGp998B1912702Q
mouse Skor2	Source Bioscience	IMAGE ID 6853809
Slc17a6 (Vglut2)	Guimera et al., 2006	n/a
Sox14	Source Bioscience	IMAGp998A2414391Q
Tal1	Source Bioscience	IRAVp968D09118D
Tal2	RZPD	IRCLp5011D0623D
Zfpm1	Source Bioscience	IMAGE ID 3585094
Zfpm2	Source Bioscience	IRAVp968B06115D
rat Skor2	see Materials and Methods	n/a